Reaction Kinetics, Mechanisms and Catalysis (2020) 129:85–94
https://doi.org/10.1007/s11144-019-01694-7

Application of carbonized ion exchange resin beads as catalyst support for gas phase hydrogenation processes

Ádám Prekob[1] · Viktória Hajdu[1] · Gábor Muránszky[1] · István Kocserha[2] · Béla Fiser[1,3] · Béla Viskolcz[1] · László Vanyorek[1]

Received: 2 October 2019 / Accepted: 26 October 2019 / Published online: 2 November 2019

Abstract

Carbonized ion exchange resin beads were prepared as catalyst for gas phase hydrogenation processes. Amberlite IR 120 polystyrene based sulfonated ion exchange beads were carbonized at 900 °C. The process of carbonization was monitored by FTIR combined thermogravimetric analysis. During the carbonization formed sulfur dioxide, carbon dioxide and organic compounds. The carbon pearls were used as catalyst support for Pd nanoparticles. The catalyst was characterized by scanning electron microscopy and X-ray diffractometry. The diameters of the palladium nanoparticles on the catalyst surface were between 15 and 50 nm, but bigger aggregates were also detected. The catalyst was tested during the gas phased heterogeneous catalytic hydrogenation of 1-butene. The hydrogenation process was followed by FTIR measurements, 93% conversion was reached after 10 min.

Keywords Resin beads · Carbonization · Gas phased hydrogenation

Introduction

Carbon based catalysts have an important role in industrial catalytic processes due to the high specific surface area [1, 2], and excellent heat conductivity [3] of the various carbon allotropes which makes them exceptional catalyst supports. Activated carbon [4], norit [5], or carbon nanotubes [6] usually decorated with catalytically active metal particles like Pd, Rh, or Pt and applied in many different reactions such as hydrocarbon oxidation [7], fuel production from biomass [8] or hydrogenation reactions. Among these, hydrogenation has far the most significant applications [9–11], particularly in case of carbon nanotube supported systems [12–14]. By

Electronic supplementary material The online version of this article (https://doi.org/10.1007/s11144-019-01694-7) contains supplementary material, which is available to authorized users.

✉ Ádám Prekob
prekob.a@gmail.com

Extended author information available on the last page of the article

applying carbon supported catalysts, the hydrogenation of nitrobenzene was successfully carried out to produce aniline [15–17]. Another important application is the gas phase hydrogenation of olefins [18, 19].

For these applications, carbon-based support materials should be created. Many different methods have already been developed for carbon material production like CVD method, ultrasonic synthesis, or electric arc technique [20–22] but one of the best methods is carbonization [23–25]. For example, activated carbon can be made by carbonizing different natural sources like bamboo chips, cherry stones, fox nut shell, sugarcane [26], coconut husk [27] and rice-straw [28]. The carbonization of ion exchange resins is another valid method to prepare carbon nanomaterials [29] and the resulted nanoporous carbon materials have a wide range of applications [30]. Singare and his colleges successfully created carbon layers from acidic cation exchange resin with thermal degradation to prepare an electrically conductive coating [31]. Zhao et al. made porous carbon support by carbonizing phenol resin and by decorating it with Pt particles the system was stable and well usable for methanol oxidation in fuel cells [32]. Other carbon nanostructure based catalysts were also tested successfully in oxidative reactions of different aromatic compounds [33–36]. Carbonized resin supports are promising materials in catalytic applications, and they have been employed in liquid phase reactions successfully [32]. However, despite their special structure, to the best of our knowledge, resin based supports have not applied in gas phase processes. For this reason, the potential catalytic application of ion exchange resin beads has been investigated and they have been carbonized and applied as catalyst support in a gas phase hydrogenation process.

Experimental

Materials and methods

Amberlite IR120 cation exchange resin (H^+ form, Sigma Aldrich) was used in the measurements. Palladium(II) nitrate dihydrate ($Pd(NO_3)_2{\cdot}2H_2O$, Merck) was applied to prepare the catalyst. Nitrogen (99.995, Messer) and hydrogen (99.9990, Messer) were used for carbonization and catalyst activation.

The process of carbonization of the Amberlite resin was followed by Fourier transform infrared spectroscopy supported with thermogravimetric analysis (FTIR–TGA). The gas cell of Bruker Vertex 70 spectrometer was combined with NETZSCH TG 209 Tarsus thermo-microbalance. The gases formed during the heat-decomposition were detected by FTIR (from 4000 to 400 cm^{-1} at 4 cm^{-1} optical resolution) depending on the heating temperature. The thermogravimetric analysis was carried out in a range of 35–900 °C, while the heating rate was 10 °C/min in synthetic air atmosphere, and the flow velocity was 20 ml/min.

The functional groups on the surface of the oxidized carbon nanotubes were determined by Bruker Vertex 70 FTIR spectroscope. All samples were investigated in potassium bromide pellets (5 mg N-BCNT in 250 mg KBr).

The different phases formed by the palladium particles on the surface of the carbon beads identified by X-ray diffraction analysis (XRD) with Rigaku Miniflex instrument (Cu K_α source).

The surface and particle morphology of the catalytic palladium particles have been characterized by scanning electron microscopy (SEM, Hitachi S 4800), while the samples were fixed with carbon tape rubber.

The sulfur, carbon, and hydrogen content of the Amberlite IR120 and the carbonized resin have been measured by Vario Macro CHNS element analyzer and the carrier gas was helium (99.9990%).

During the catalyst preparation, palladium nanoparticles were deposited onto the surface of the carbonized resin pearls. The carbon beads (12 g) were impregnated by 15 ml 2 wt% palladium solution (1 g $Pd(NO_3)_2 \cdot 2H_2O$ in 50 ml water) which was added to 100 ml distilled water. The water was evaporated and the carbon beads impregnated with Pd were dried at 120 °C overnight. The impregnated beads were heat-treated in nitrogen flow at 400 °C for 20 min. Then, to form catalytically active Pd nanoparticles on the surface of the beads, the system was hydrogenated at 400 °C for 30 min.

Catalytic activity of the samples was tested in 1-butene hydrogenation and followed by FTIR spectroscopy using a quartz tube reactor (tube OD: 10 mm) which is coupled to the gas cell of the FTIR instrument (Fig. 1). The vibration of the C=C double bonds in olefins like 1-butene can be detected at 1642 cm^{-1} and during hydrogenation the intensity of the peaks decreasing. Based on the areas of the bands, the conversions were calculated. The FTIR was calibrated with the H_2/N_2/1-butene gas mixture by using four different 1-butene concentrations, at room temperature and atmospheric pressure. The spectra were measured three times (every 10 min) in each case (Supplementary Information). During the tests 0.5 g catalyst was used at 50 °C reaction temperature. For the measurements nitrogen (40 ml/min), hydrogen (40 ml/min) and 1-butene (20 ml/min) was added to the system at atmospheric

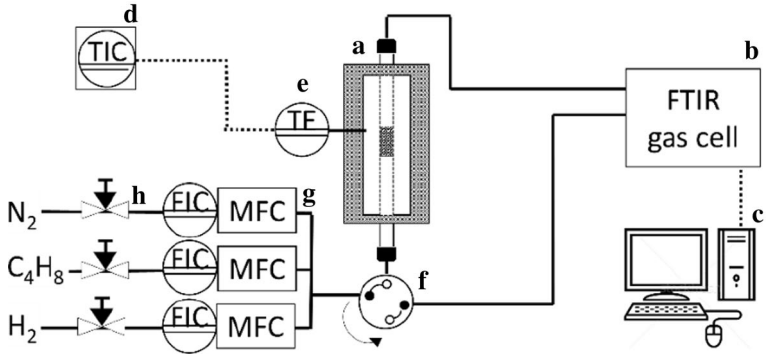

Fig. 1 Experimental setup to measure the catalytic activity of the catalyst in gas phase hydrogenation: *a* reactor with the catalyst in tube furnace, *b*, *c* FTIR instrument connected to a computer, *d*, *e* temperature indicator controller (TIC) with thermocouple, *f* four-way valve for gas inlet into the reactor and the FTIR gas cell, *g* mass flow meter and controller, *h* valves for the gases

pressure. The molar ratio of the hydrogen to 1-butene was 2:1 and weight hour space velocity (WHSV) was 5.49 kg 1-butene/1 kg catalyst per hour.

The system was calibrated for five different 1-butene concentrations to ensure a linear quantitative response.

The efficacy of the catalytic hydrogenation was measured by the conversion (X%) of 1-butene based on the following equation (Eq. 1):

$$X\% = \frac{\text{consumed } n_{\text{1-butene}}}{\text{initial } n_{\text{1-butene}}} \times 100 \quad (1)$$

Results

First step of the catalyst preparation: decomposition of the ion exchange resin measured by FTIR–TGA

The carbonization process was followed by FTIR–TGA. Different gases have been formed depending on the applied temperature (Fig. 2a, b). The presence of water is indicated by the βOH and νOH vibration bands at ~ 1400 cm^{-1} and ~ 3500 cm^{-1} (Fig. 2b). The dehydration of the carbon pearls started around 85 °C. The adsorbed water which was 20 wt% has been eliminated when the temperature reached 510 °C (Fig. 2a). In the meantime, the CO_2 formation (oxidation of carbon) started due to the oxygen elimination from various functional groups (e.g. $–SO_3H$) at 382 °C and indicated by the asymmetric stretching and bending vibration mode of carbon dioxide appeared at ~ 2560 cm^{-1} and 520 cm^{-1}. A great amount of the sulfur content released at 220 °C, which resulted an adsorption band with high intensity at ~ 1370 cm^{-1}. Organic compounds are eliminated after reaching 500 °C, shown by the bands at ~ 2980 cm^{-1}, and the weight loss was 7.9 wt%, which included the release of sulfur in the form of SO_2.

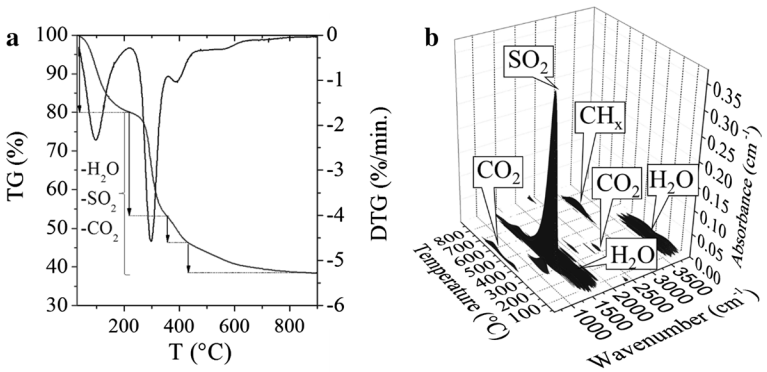

Fig. 2 TG-DTG curves of the carbonization of Amberlite IR120 (**a**), and FTIR spectra of the gases formed during the process (**b**)

Table 1 Results of the elemental analysis of the Amberlite IR120 resin and its carbonized counterpart

	Sulfur (wt%)	Carbon (wt%)	Hydrogen (wt%)
Amberlite IR 120	18.38	51.64	4.73
Carbonized resin	6.42	93.10	0.57

Sulfur, carbon and hydrogen contents are given

The dried Amberlite resin was measured with CHNS elemental analyzer (Table 1). The initial sulfur content before thermal decomposition was 18.38 wt%, which decreased to 6.42 wt% after the heat-treatment at 900 °C.

FTIR analysis of the non-carbonized and the carbonized ion exchange resin

The Amberlite IR120 ion exchange resin was examined by using FTIR spectroscopy before and after carbonization in order to determine the accessible functional groups in the samples (Fig. 3a, b). On the spectra of the initial amberlite beads and their carbonized form, the bands of the stretching mode of C–H groups can be found between 2860 and 2930 cm^{-1}, which can be associated with the polymeric matrix of styrene [37, 38]. The band at ~ 1630 cm^{-1} assigned to the vibration of benzene ring [37, 38]. Stretching mode of the hydroxyl groups are shown on the spectra around 3400 cm^{-1}. The bands observed at 1222 cm^{-1} and 1413 cm^{-1} in the case of the Ambelite IR120 resin, are assigned to the symmetric and asymmetric stretching vibration of the $–SO_2$ group of sulfonic acid (Fig. 3a). Four peaks are found on the spectrum of the non-carbonized resin at 1002 cm^{-1}, 1038 cm^{-1}, 1134 cm^{-1}, and 1158 cm^{-1} which indicates the presence of sulfonic acid groups (Fig. 3a). After the carbonization process, some bands in the region of 1000–1200 cm^{-1} are disappeared, due to the significant decrease of the sulfur content and the elimination of $–SO_3H$ groups (Fig. 3b). The carbon content does not leave completely the carbon matrix, but create $R–SO_2–R$ and R–S=O bonds, which leads to the appearance of bands at 1118 cm^{-1}, 1389 cm^{-1}, and 1038 cm^{-1}.

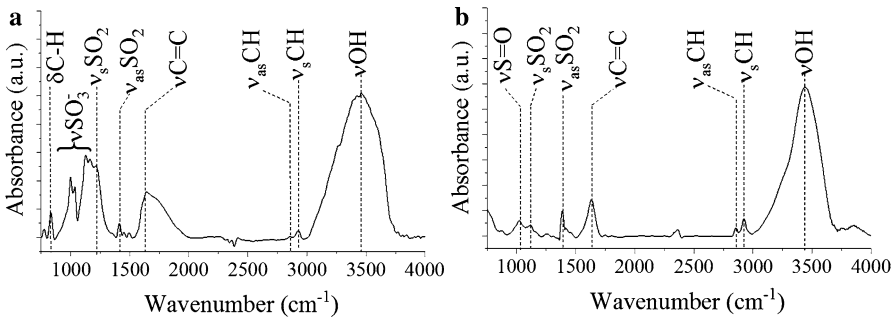

Fig. 3 FTIR spectra of Amberlite IR120 (**a**), and the carbonized resin (**b**)

Second step of the catalyst preparation: deposition of Pd nanoparticles on the surface of the carbonized resin have been proved by XRD results

In the XRD pattern of the carbonized resin beads two forms of carbon were detected, at 24.5° and 43.1° 2θ, which were identified as the C(002) and C(101) reflections (Fig. 4). The carbon pearls were not contained any other inorganic crystal phases. On the diffractograms of the catalyst, the typical reflections of the elemental palladium were shown, such as Pd(111), Pd(200), Pd(220), Pd(311), and Pd(222) at 40.2°; 46.5°; 68.2°, 82.2°, and 86.5° 2θ. (Fig. 4b). Thus, the hydrogenation step of catalyst preparation was efficient and palladium nanoparticles have been deposited on the surface of the carbonized resin.

Surface characterization of the Pd catalyst based on SEM–EDS results

In the SEM images the carbonated resin and the Pd nanoparticles with different magnifications could be detected (Fig. 5a–c). The Pd nanoparticles were prepared with high dispersity on the surface of the spheres, their diameters were mostly between 15 nm and 50 nm. However, bigger aggregates were also detected. The presence of Pd and C were verified by energy-dispersive X-ray (EDS) spectroscopy (Fig. 5d), and the peak of the sulfur could be also seen, as it was detected by FTIR and CHNS analysis methods.

Catalytic test of the Pd/carbonized resin catalyst

Despite of the 6.42 wt% sulfur content, the carbonized ion exchange resin supported Pd catalyst was catalytically active during the hydrogenation of 1-butene. After 5 min, the conversion reached 93% and stayed at that value (Fig. 6). The high conversion value despite of the sulfur content proved that the catalyst could be promising in gas phase hydrogenation reactions.

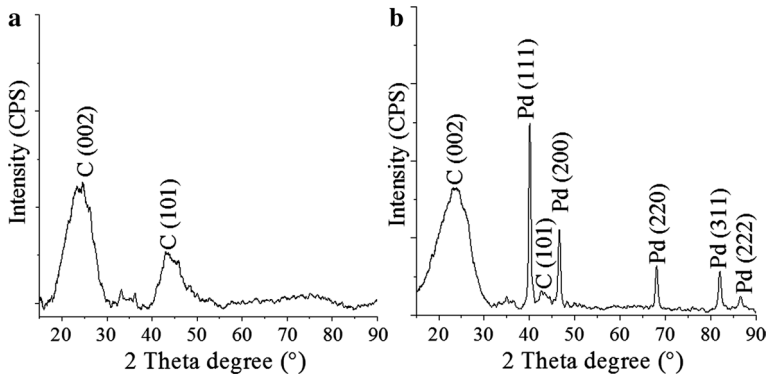

Fig. 4 XRD patterns of the carbonized resin beads (**a**) and the palladium containing catalyst (**b**)

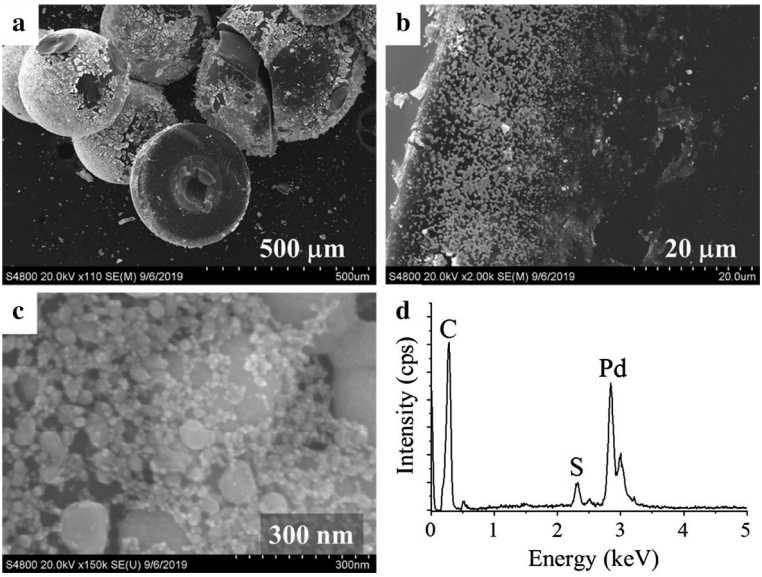

Fig. 5 SEM images (**a**, **b**, **c**) and EDS spectra (**d**) of the Pd/carbonized resin catalyst

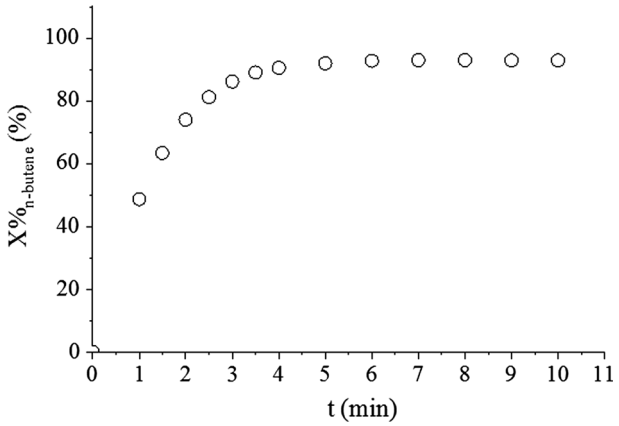

Fig. 6 1-butene conversion *vs* time of hydrogenation

Conclusion

Carbon beads were synthesized from polystyrene based ion exchange resin pearls. The carbonization process was followed by FTIR–TGA measurements. On the surface of the carbon beads several hydroxyl groups were detected, which were applicable for the anchoring of catalytically active metal ions. The presence of hydroxyl groups on the surface of the beads makes them easily wettable in the aqueous phase of catalytic metal precursors. The activation step (reduction in H_2) of the palladium

precursor impregnated carbon beads was efficient based on the XRD results, and it was similar to the conventional catalyst activation. On the surface of the catalyst, palladium nanoparticles were identified in homogeneous dispersibility with small particle size (the average diameter was 39 nm). The prepared Pd/carbonized resin catalyst was successfully tested in 1-butene hydrogenation. High catalytic activity was achieved (93% conversion). By the carbonization of ion exchange resin beads, excellent catalyst support materials could be produced, which are easily applicable in gas phased hydrogenation of olefins.

Acknowledgements Open access funding provided by University of Miskolc (ME). This research was supported by the European Union and the Hungarian State, co-financed by the European Regional Development Fund in the framework of the GINOP-2.3.4-15-2016-00004 project, aimed to promote the cooperation between the higher education and the industry.

Compliance with ethical standards

Conflict of interest On behalf of all authors, the corresponding author states that there is no conflict of interest.

References

1. Cao Q, Xie K-C, Lv Y-K, Bao W-R (2006) Process effects on activated carbon with large specific surface area from corn cob. Bioresour Technol 97:110–115. https://doi.org/10.1016/J.BIORTECH.2005.02.026
2. Peigney A, Laurent C, Flahaut E et al (2001) Specific surface area of carbon nanotubes and bundles of carbon nanotubes. Carbon 39:507–514. https://doi.org/10.1016/S0008-6223(00)00155-X
3. Popov VN (2004) Carbon nanotubes: properties and application. Mater Sci Eng 43:61–102. https://doi.org/10.1016/J.MSER.2003.10.001
4. Jüntgen H (1986) Activated carbon as catalyst support: a review of new research results. Fuel 65:1436–1446. https://doi.org/10.1016/0016-2361(86)90120-1
5. Tolmacsov P, Gazsi A, Solymosi F (2009) Decomposition and reforming of methanol on Pt metals supported by carbon Norit. Appl Catal A Gen 362:58–61. https://doi.org/10.1016/J.APCATA.2009.04.015
6. Sikora E, Prekob Á, Halasi G et al (2018) Development and application of carbon-layer-stabilized, nitrogen-doped, bamboo-like carbon nanotube catalysts in CO_2 Hydrogenation. ChemistryOpen 7:789–796. https://doi.org/10.1002/open.201800162
7. Xiong H, Wiebenga MH, Carrillo C et al (2018) Design considerations for low-temperature hydrocarbon oxidation reactions on Pd based catalysts. Appl Catal B 236:436–444. https://doi.org/10.1016/J.APCATB.2018.05.049
8. Lam E, Luong JHT (2014) Carbon materials as catalyst supports and catalysts in the transformation of biomass to fuels and chemicals. ACS Catal 4:3393–3410. https://doi.org/10.1021/cs5008393
9. Díaz E, Mohedano AF, Calvo L et al (2007) Hydrogenation of phenol in aqueous phase with palladium on activated carbon catalysts. Chem Eng J 131:65–71. https://doi.org/10.1016/J.CEJ.2006.12.020
10. Yoshinaga Y, Akita T, Mikami I, Okuhara T (2002) Hydrogenation of nitrate in water to nitrogen over Pd–Cu supported on active carbon. J Catal 207:37–45. https://doi.org/10.1006/JCAT.2002.3529

11. Vanyorek L, Halasi G, Pekker P et al (2016) Characterization and catalytic activity of different carbon supported Pd nanocomposites. Catal Lett 146:2268–2277. https://doi.org/10.1007/s10562-016-1857-8
12. Jin S, Qian W, Liu Y et al (2010) Granulated carbon nanotubes as the catalyst support for Pt for the hydrogenation of nitrobenzene. Aust J Chem 63:131–134. https://doi.org/10.1071/CH09162
13. Li C-H, Yu Z-X, Yao K-F et al (2005) Nitrobenzene hydrogenation with carbon nanotube-supported platinum catalyst under mild conditions. J Mol Catal A 226:101–105. https://doi.org/10.1016/J.MOLCATA.2004.09.046
14. Liang X-L, Dong X, Lin G-D, Zhang H-B (2009) Carbon nanotube-supported Pd–ZnO catalyst for hydrogenation of CO_2 to methanol. Appl Catal B 88:315–322. https://doi.org/10.1016/J.APCATB.2008.11.018
15. Wu S, Wen G, Zhong B et al (2014) Reduction of nitrobenzene catalyzed by carbon materials. Chin J Catal 35:914–921. https://doi.org/10.1016/S1872-2067(14)60102-9
16. Srikanth CS, Kumar VP, Viswanadham B et al (2015) Vapor phase hydrogenation of nitrobenzene to aniline over carbon supported ruthenium catalysts. J Nanosci Nanotechnol 15:5403–5409. https://doi.org/10.1166/jnn.2015.9872
17. Prekob Á, Muránszky G, Hutkai ZG et al (2018) Hydrogenation of nitrobenzene over a composite catalyst based on zeolite supported N-doped carbon nanotubes decorated with palladium. Reac Kinet Mech Cat 125:583–593. https://doi.org/10.1007/s11144-018-1481-2
18. Hill T, Haake M, Schwab E et al (2002) Selective catalytic gas-phase hydrogenation of alkynes, dienes, alkenynes and/or polyenes. Patent No.: US20030069458A1
19. Vanyorek L, Prekob Á, Baráth M et al (2019) Development of nitrogen-doped bamboo-like carbon nanotubes coated zeolite beads as support on support catalyst for the catalytic hydrogenation of olefins. Reac Kinet Mech Cat. https://doi.org/10.1007/s11144-019-01592-y
20. Li H, He X, Liu Y et al (2011) One-step ultrasonic synthesis of water-soluble carbon nanoparticles with excellent photoluminescent properties. Carbon 49:605–609. https://doi.org/10.1016/J.CARBON.2010.10.004
21. Koziol K, Boskovic BO, Yahya N (2010) Synthesis of carbon nanostructures by CVD method. Springer, Berlin, pp 23–49
22. Journet C, Maser WK, Bernier P et al (1997) Large-scale production of single-walled carbon nanotubes by the electric-arc technique. Nature 388:756–758. https://doi.org/10.1038/41972
23. Sevilla M, Fuertes AB (2009) The production of carbon materials by hydrothermal carbonization of cellulose. Carbon 47:2281–2289. https://doi.org/10.1016/J.CARBON.2009.04.026
24. Rozlívková Z, Trchová M, Exnerová M, Stejskal J (2011) The carbonization of granular polyaniline to produce nitrogen-containing carbon. Synth Met 161:1122–1129. https://doi.org/10.1016/J.SYNTHMET.2011.03.034
25. Rajesh B, Ravindranathan Thampi K, Bonard J-M et al (2003) Carbon nanotubes generated from template carbonization of polyphenyl acetylene as the support for electrooxidation of methanol. J Phys Chem 107:2701–2708. https://doi.org/10.1021/JP0219350
26. Thomas BN, George SC (2015) Production of activated carbon from natural sources. iMedPub J Trends Green Chem 1:1–5
27. Tan IAW, Ahmad AL, Hameed BH (2008) Optimization of preparation conditions for activated carbons from coconut husk using response surface methodology. Chem Eng J 137:462–470. https://doi.org/10.1016/J.CEJ.2007.04.031
28. Oh GH, Park CR (2002) Preparation and characteristics of rice-straw-based porous carbons with high adsorption capacity. Fuel 81:327–336. https://doi.org/10.1016/S0016-2361(01)00171-5
29. Le T-H, Yoon H (2019) Strategies for fabricating versatile carbon nanomaterials from polymer precursors. Carbon 152:796–817. https://doi.org/10.1016/J.CARBON.2019.06.053
30. Prasetyo I, Rochmadi R, Ariyanto T, Yunanto R (2013) Simple method to produce nanoporous carbon for various applications by pyrolysis of specially synthesized phenolic resin. Indones J Chem 13:95–100. https://doi.org/10.22146/ijc.21290
31. Singare PU, Lokhande RS, Madyal RS (2011) Thermal degradation studies of some strongly acidic cation exchange resins. Open J Phys Chem 01:45–54. https://doi.org/10.4236/ojpc.2011.12007
32. Zhao J, Cheng F, Yi C et al (2009) Facile synthesis of hierarchically porous carbons and their application as a catalyst support for methanol oxidation. J Mater Chem 19:4108. https://doi.org/10.1039/b821216n

33. Wang R, Li B, Xiao Y et al (2018) Optimizing Pd and Au-Pd decorated Bi_2WO_6 ultrathin nanosheets for photocatalytic selective oxidation of aromatic alcohols. J Catal 364:154–165. https://doi.org/10.1016/j.jcat.2018.05.015
34. Li B, Shao L, Wang R et al (2018) Interfacial synergism of Pd-decorated BiOCl ultrathin nanosheets for the selective oxidation of aromatic alcohols. J Mater Chem A 6:6344–6355. https://doi.org/10.1039/c8ta00449h
35. Tao X, Shao L, Wang R et al (2019) Synthesis of BiVO 4 nanoflakes decorated with AuPd nanoparticles as selective oxidation photocatalysts. J Colloid Interface Sci 541:300–311. https://doi.org/10.1016/j.jcis.2019.01.108
36. Wang R, Qiu G, Xiao Y et al (2019) Optimal construction of $WO_3{\cdot}H_2O$/Pd/CdS ternary Z-scheme photocatalyst with remarkably enhanced performance for oxidative coupling of benzylamines. J Catal. https://doi.org/10.1016/j.jcat.2019.05.016
37. Smith BC (1999) Infrared spectral interpretation : a systematic approach. CRC Press, Boca Raton
38. Cortina JL, Miralles N, Aguilar M, Sastre AM (1994) Extraction studies of Zn(II), Cu(II) and Cd(II) with impregnated and Levextrel resins containing di(2-ethylhexyl) phosphoric acid (Lewatit 1026 Oc). Hydrometallurgy 36:131–142. https://doi.org/10.1016/0304-386X(94)90001-9

Affiliations

Ádám Prekob[1] · Viktória Hajdu[1] · Gábor Muránszky[1] · István Kocserha[2] · Béla Fiser[1,3] · Béla Viskolcz[1] · László Vanyorek[1]

Viktória Hajdu
kemviki@uni-miskolc.hu

Gábor Muránszky
kemmug@uni-miskolc.hu

István Kocserha
istvan.kocserha@uni-miskolc.hu

Béla Fiser
fiser.bela@gmail.com

Béla Viskolcz
bela.viskolcz@uni-miskolc.hu

László Vanyorek
kemvanyi@uni-miskolc.hu

[1] Institute of Chemistry, University of Miskolc, Miskolc, Miskolc-Egyetemváros 3515, Hungary

[2] Institute of Ceramic and Polymer Engineering, University of Miskolc, Miskolc, Miskolc-Egyetemváros 3515, Hungary

[3] Ferenc Rákóczi II. Transcarpathian Hungarian Institute, Beregszász, Transcarpathia 90200, Ukraine